
ParamMute: Suppressing Knowledge-Critical FFNs for Faithful Retrieval-Augmented Generation

Pengcheng Huang¹, Zhenghao Liu^{1*}, Yukun Yan², Haiyan Zhao², Xiaoyuan Yi³, Hao Chen², Zhiyuan Liu², Maosong Sun², Tong Xiao¹, Ge Yu¹, Chenyan Xiong⁴

¹School of Computer Science and Engineering, Northeastern University, China

²Department of Computer Science and Technology, Institute for AI, Tsinghua University, China

³Microsoft Research Asia, Beijing, China

⁴Language Technologies Institute, Carnegie Mellon University, United States

Abstract

Large language models (LLMs) integrated with retrieval-augmented generation (RAG) have improved factuality by grounding outputs in external evidence. However, they remain susceptible to unfaithful generation, where outputs contradict retrieved context despite its relevance and accuracy. Existing approaches aiming to improve faithfulness primarily focus on enhancing the utilization of external context, but often overlook the persistent influence of internal parametric knowledge during generation. In this work, we investigate the internal mechanisms behind unfaithful generation and identify a subset of mid-to-deep feed-forward networks (FFNs) that are disproportionately activated in such cases. Building on this insight, we propose Parametric Knowledge Muting through FFN Suppression (ParamMute), a framework that improves contextual faithfulness by suppressing the activation of unfaithfulness-associated FFNs and calibrating the model toward retrieved knowledge. To evaluate our approach, we introduce CoFaithfulQA, a benchmark specifically designed to evaluate faithfulness in scenarios where internal knowledge conflicts with accurate external evidence. Experimental results show that ParamMute significantly enhances faithfulness across both CoFaithfulQA and the established ConFiQA benchmark, achieving substantial reductions in reliance on parametric memory. These findings underscore the importance of mitigating internal knowledge dominance and provide a new direction for improving LLM trustworthiness in RAG. All codes are available at <https://github.com/OpenBMB/ParamMute>.

1 Introduction

Large language models (LLMs), such as GPT-4 [39] and LLaMA [47], have demonstrated exceptional performance across a wide range of natural language processing tasks [52, 62]. Nonetheless, they are known to suffer from hallucinations, frequently generating factually incorrect or fabricated information [10, 20]. To address this, retrieval-augmented generation (RAG) has emerged as a promising paradigm, grounding model outputs in external evidence to improve factual accuracy [29, 61]. Despite these advancements, recent studies [1, 34] have identified a persistent and subtle challenge: LLMs may still produce unfaithful responses that contradict or disregard external evidence even when this evidence is accurate and highly relevant [34, 54]. Such unfaithful generation can significantly undermine the reliability of RAG systems [21].

Recent approaches primarily seek to improve contextual faithfulness by enhancing the model’s ability to incorporate external evidence—either through advanced prompting strategies [22, 63] or context-

* indicates corresponding author.

aware decoding techniques [1, 18]. However, these externally focused methods often overlook the role of internal knowledge in undermining generation faithfulness. Motivated by this gap, we turn our attention to examining how parametric knowledge influences the generation process. Specifically, we focus on the feed-forward networks (FFNs) within Transformer-based LLMs, which are widely recognized as key repositories of memorized knowledge [7, 15]. Indeed, our pilot study reveals that when a specific subset of mid-to-deep FFN layers exhibits excessive activation, the model tends to rely more heavily on its internal knowledge, consequently producing unfaithful outputs.

Building on this observation, we propose Parametric Knowledge Muting through FFN Suppression (ParamMute), a novel framework designed to enhance the contextual faithfulness of LLMs. Specifically, ParamMute first identifies the FFN layers most associated with unfaithful generation and suppresses their activation to mitigate the undue influence of internal knowledge. A plug-and-play knowledge preference calibration module is then applied to the suppressed LLM to further encourage reliance on external evidence, ultimately yielding more trustworthy responses.

Additionally, to reliably evaluate LLM faithfulness, we introduce CoFaithfulQA, a comprehensive benchmark built from six open-domain QA datasets. It focuses on realistic scenarios where model responses may conflict with accurate retrieved evidence. Experimental results demonstrate that ParamMute consistently outperforms strong baselines on both CoFaithfulQA and the established ConFiQA benchmark [1]. It improves faithfulness by an average of 6.17% and 54.63% on the two benchmarks, respectively, while substantially reducing reliance on parametric knowledge. These results highlight the importance of explicitly accounting for internal knowledge as a key step toward building more faithful and trustworthy language models.

2 Preliminaries: Understanding the Role of FFN in Unfaithful Generation

In this work, we aim to investigate the influence of internal knowledge on unfaithful generation. To explore this, we focus on feed-forward networks, which interpretability studies have identified as primary repositories of parametric knowledge [16, 59]. This makes them ideal targets for analyzing the role of internal knowledge in unfaithful generation. This section begins by outlining the foundational concepts of knowledge representation and neuron activation in LLMs. We then conduct an empirical analysis using FFN activation patterns as a proxy for internal knowledge utilization, aiming to investigate their correlation with unfaithful model outputs.

2.1 Background: FFNs as Knowledge Carriers and Activation Analysis

Feed-Forward Networks as Parametric Knowledge Stores. Recent interpretability studies have shown that FFNs function similarly to key-value memory mechanisms, storing the majority of the parametric knowledge [15] through two parameter matrices $\mathbf{K}, \mathbf{V} \in \mathbb{R}^{d_m \times d}$, where d_m and d are the dimensions of the intermediate and input representations, respectively. For the i -th token in the input sequence, the FFN processes its representation $\mathbf{x}_i \in \mathbb{R}^d$ from the last layer through linear transformations. Formally, the computation in the l -th FFN can be expressed as a key-value memory mechanism:

$$\text{FFN}(\mathbf{x}_i^l) = (\sigma(\mathbf{K}^l \mathbf{x}_i^l))^\top \mathbf{V}^l, \quad (1)$$

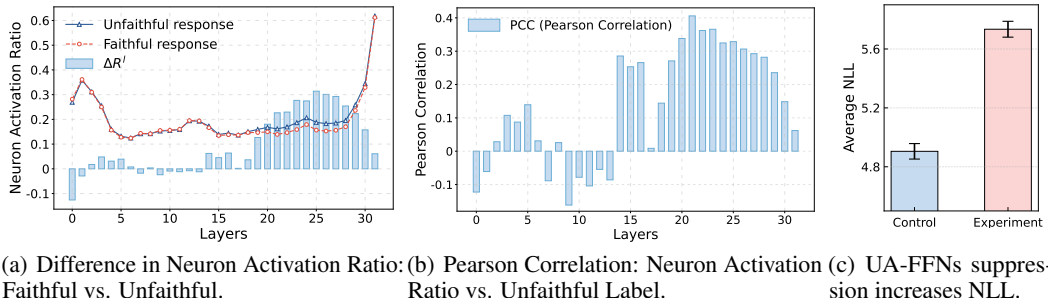
where σ is the activation function. Geva et al. [15] further show that the FFN output can be expressed as a weighted sum over a set of value vectors:

$$\text{FFN}(\mathbf{x}_i^l) = \sum_{j=1}^{d_m} \sigma(\mathbf{x}_i^l \cdot \mathbf{k}_j^l) \mathbf{v}_j^l = \sum_{j=1}^{d_m} a_{ij}^l \mathbf{v}_j^l, \quad (2)$$

where \mathbf{k}_j^l and \mathbf{v}_j^l denote the j -th row of \mathbf{K}^l (the subkey) and the j -th column of \mathbf{V}^l (the subvalue), respectively. The term $a_{ij}^l = \sigma(\mathbf{x}_i^l \cdot \mathbf{k}_j^l)$ represents the *activation coefficient* associated with the neuron \mathbf{v}_j^l . Following Mu et al. [37], we consider a neuron *activated* when a_{ij}^l exceeds zero.

Activation-based Metric. Since each activated FFN neuron contributes independently to the final output [15, 16], we can quantify the overall activation level through an *activation ratio*. For a token representation \mathbf{x}_i^l at layer l , the activation ratio $R^l(\mathbf{x}_i^l)$ at layer l is defined as the fraction of neurons that are activated:

$$R^l(\mathbf{x}_i^l) = \frac{1}{d_m} \sum_{j=1}^{d_m} \mathbb{I}[a_{ij}^l], \quad (3)$$



(a) Difference in Neuron Activation Ratio: (b) Pearson Correlation: (c) UA-FFNs suppression increases NLL.
Faithful vs. Unfaithful. Neuron Activation Ratio vs. Unfaithful Label.

Figure 1: Activation Pattern Differences and Causal Impact on Unfaithfulness. (a) Activation ratio comparison between faithful and unfaithful generations. (b) Pearson correlation between unfaithfulness and FFN activation ratio, with UA-FFNs layers highlighted. (c) Suppressing UA-FFNs increases the Negative Log-Likelihood Loss (NLL) on unfaithful data, indicating a causal role.

where $\mathbb{I}[a_{ij}^l]$ is an indicator function that returns 1 if $a_{ij}^l > 0$, and 0 otherwise. Intuitively, a higher $R^l(x_i^l)$ indicates that more neurons in the FFN are actively participating in computing the output, reflecting a greater involvement of parametric knowledge stored in the FFN layer [11, 15, 59]. We compute the response-level activation ratio by averaging the activation ratios over all tokens in the response $\hat{r} = \{r_1, \dots, r_T\}$:

$$R^l(\hat{r}) = \frac{1}{T} \sum_{i=1}^T R^l(r_i^l). \quad (4)$$

2.2 Pilot Study: Are Certain FFNs Implicated in Unfaithful Generation?

Building on the activation-based analysis framework introduced above, we now conduct an empirical investigation into a key hypothesis: *Do unfaithful responses correspond to disproportionately high activation in certain FFN layers?*

Dataset for Activation Analysis. To support this analysis, we use the proposed benchmark CoFaithfulQA, denoted as \mathcal{D} , which consists of model-generated responses annotated with binary faithfulness labels. These annotations enable direct comparison of activation patterns between faithful and unfaithful generations. Each instance $(q, c, y^*, \hat{r}, y_f) \in \mathcal{D}$ includes an input query q , a retrieved context c , a ground-truth answer y^* derived from the evidence c , a model-generated response \hat{r} , and a binary label $y_f \in \{0, 1\}$, indicating whether \hat{r} is faithful to the context c (see Section 4 for construction and annotation details). For comparative analysis, we partition \mathcal{D} into a faithful subset \mathcal{D}^+ and an unfaithful subset \mathcal{D}^- based on the faithfulness label y_f . We then analyze the FFN activation patterns of the LLaMA3-8B-Instruct model across the two groups to investigate how activation behavior differs between faithful and unfaithful generations.

Activation Differences Between Faithful and Unfaithful Responses. To quantitatively examine the relationship between FFN activation and response faithfulness, we compute the layer-wise activation ratio $R^l(\hat{r})$, as defined in Eq. 4, for both the unfaithful subset \mathcal{D}^- and the faithful subset \mathcal{D}^+ . We then define their difference as the *activation gap*, given by:

$$\Delta R^l = \mathbb{E}_{\mathcal{D}^-}[R^l(\hat{r})] - \mathbb{E}_{\mathcal{D}^+}[R^l(\hat{r})] \quad (5)$$

As shown in Figure 1(a), while most FFN layers exhibit minimal differences, we observe consistently higher activation in \mathcal{D}^- within a narrow range of layers, particularly in the middle-to-deep transformer blocks (i.e., layers 20 to 29). This pattern suggests that unfaithful generations may be associated with distinct activation behaviors concentrated in these specific layers.

Correlation and Causal Analysis of FFN Activation for Unfaithful Generation. To statistically verify this association, we compute the Pearson Correlation Coefficient (PCC) between the activation ratio $R^l(\hat{r})$ and the unfaithfulness indicator $(1 - y_f)$ across the dataset. As shown in Figure 1(b), mid-to-deep FFN layers exhibit increasingly positive correlations (p -value < 0.05), confirming a significant positive correlation between activation in these layers and unfaithful generation. This evidence supports our hypothesis that a specific subset of mid-to-deep FFN layers—termed *Unfaithfulness-Associated FFNs* (UA-FFNs)—plays a central role in unfaithful generation. When these layers exhibit

excessive activation, the model increasingly relies on internal parametric knowledge (as further evidenced in Appendix A.11), overriding retrieved context and leading to unfaithful outputs.

To examine whether the observed correlation reflects a causal relationship, we perform a causal intervention [13] by suppressing the activation of selected FFN layers. Specifically, we compare the Negative Log-Likelihood (NLL) loss between an experimental group (with suppressed UA-FFNs) and a control group (using the vanilla model) on the unfaithful subset \mathcal{D}^- . The detailed intervention procedures are described in Appendix A.3. As shown in Figure 1(c), the experimental group exhibits consistently higher NLL than the control group, as expected—indicating that suppression of UA-FFNs makes unfaithful responses harder to generate. These results provide causal evidence that the activation strength of UA-FFNs directly influences the likelihood of unfaithful generation.

Summary and Implications. Our pilot study reveals that unfaithful generation in LLMs is associated with the over-reliance on internal parametric knowledge through UA-FFNs. Motivated by this, ParamMute (§3) applies selective suppression to UA-FFNs activations to limit parametric knowledge expression and improve contextual faithfulness.

3 Methodology

In this section, we present **Parametric Knowledge Muting** through FFN Suppression (ParamMute), a two-stage framework for improving the contextual faithfulness of LLMs. ParamMute first mitigates the influence of parametric knowledge by suppressing the activation of UA-FFNs (§3.1), and then incorporates an adaptation module to promote reliance on external knowledge (§3.2).

3.1 Reducing Internal Knowledge Reliance via Activation Suppression

Our pilot study in Section 2.2 reveals that unfaithful responses tend to involve a greater degree of internal parametric knowledge within a specific subset of FFNs (UA-FFNs). Motivated by this finding, we propose to suppress the activation of UA-FFNs, aiming to reduce the influence of internal knowledge and thereby enhance contextual faithfulness. Formally, for each layer l , we compute the average activation ratio $R^l(\hat{r})$ on both the unfaithful subset \mathcal{D}^- and the faithful subset \mathcal{D}^+ . We then use the previously defined activation gap ΔR^l (Eq. 5) to capture the difference in FFN activation between unfaithful and faithful outputs. Finally, we rank all layers \mathbb{L} by their corresponding ΔR^l and select the top- N layers with the highest activation gaps for subsequent suppression:

$$L_{\text{sup}} = \{l \in \mathbb{L} \mid l \text{ ranks in Top-}N \text{ of } \Delta R^l\}. \quad (6)$$

A suppression coefficient $\lambda \in [0, 1]$ is introduced to reduce the activation of UA-FFNs. Accordingly, the original FFN computation (Eq. 1) is reformulated as:

$$\text{FFN}^l(\mathbf{x}_i^l) = (\lambda \cdot \sigma(\mathbf{K}^l \mathbf{x}_i^l))^{\top} \mathbf{V}^l, \quad \text{if } l \in L_{\text{sup}}. \quad (7)$$

Setting $\lambda = 1$ restores the model’s original behavior. As λ decreases, the contribution of the selected FFNs is progressively reduced. When $\lambda = 0$, the suppressed FFNs are fully deactivated and no longer influence the model’s output. This soft suppression mechanism enables fine-grained control over the contribution of internal parametric knowledge.

3.2 Knowledge-Augmented Adaptation through Preference Optimization

After suppression, we further incorporate a plug-and-play adaptation module [19] to recalibrate the model’s knowledge utilization preferences, enabling more effective usage of external evidence.

$$\mathcal{L} = \sum_D \alpha \cdot \mathcal{L}_{\text{KAT}} + \beta \cdot \mathcal{L}_{\text{KPO}}, \quad (8)$$

where D denotes the set of all training instances, each comprising a query q , a retrieved context c , and a ground-truth answer y^* ; and α and β are hyperparameters that control the balance between the two objectives. The Knowledge-Augmented Training (\mathcal{L}_{KAT}) and Knowledge Preference Optimization (\mathcal{L}_{KPO}) objectives guide the suppressed model to both generate accurate answers and calibrate its knowledge usage preference towards external knowledge.

Knowledge-Augmented Finetuning. Following Lin et al. [33], we maximize the likelihood of generating the ground truth answer y^* based on both query q and external knowledge c :

$$\mathcal{L}_{\text{KAT}} = -\log P(y^* \mid q, c), \quad (9)$$

This objective trains the suppressed model to leverage both internal and external knowledge to answer the question accurately.

Knowledge Preference Optimization. To further refine the model’s reliance on external versus internal knowledge, we apply a max-margin loss [8] to optimize the likelihood of generating ground truth answers that depend more on external knowledge:

$$\mathcal{L}_{\text{KPO}} = [\gamma - \log P(y^* | q, c) + \log P(y^* | q)]_+, \quad (10)$$

where γ is a margin parameter that controls the preference constraint, and the $[.]_+$ function ensures non-negativity. This objective further finetunes the suppressed model to shift its reliance towards external knowledge, improving the reliability and faithfulness of its responses.

4 CoFaithfulQA: A Consistency-Filtered Contextual Faithfulness QA Dataset

In this section, we introduce **Consistency-filtered Contextual Faithfulness QA** (CoFaithfulQA), a benchmark designed to evaluate the faithfulness of LLMs, and present the data collection pipeline along with the manual effort involved in constructing CoFaithfulQA.

Characteristics of CoFaithfulQA. Evaluating contextual faithfulness requires scenarios in which external evidence should override a model’s incorrect internal knowledge. However, prior work has primarily relied on synthetic counterfactual contexts that contradict known correct answers [34, 45, 53]. While effective for controlled testing, such synthetic settings often fail to reflect the naturally occurring inconsistencies between retrieved evidence and model responses that commonly arise in real-world applications.

Data Collection and Processing Pipeline. Our CoFaithfulQA is constructed from six widely-used open-domain QA datasets: Natural Questions (NQ) [27], SQuAD [41], NewsQA [48], TriviaQA [25], SearchQA [9], and HotpotQA [56]. These datasets span a diverse range of domains, question types, and reasoning requirements, collectively forming a comprehensive evaluation testbed. Each QA triplet $(q, c, y^*) \in \mathcal{D}$ consists of the query q , relevant evidence c and the ground truth y^* . Then the QA triplet is augmented as $(q, c, y^*, \hat{r}, y_f)$ with a model-generated response \hat{r} and a faithfulness label y_f , based on which we form the subsets of CoFaithfulQA, \mathcal{D}^- ($y_f = 0$) and \mathcal{D}^+ ($y_f = 1$).

To facilitate the evaluation of LLM faithfulness, CoFaithfulQA is constructed to reflect realistic scenarios where models are expected to rely on accurate external evidence rather than incorrect parametric knowledge. Specifically, we employ a two-stage pipeline: we first extract the model’s dominant parametric knowledge through self-consistency filtering, and then identify conflicts between this belief and retrieved evidence using multi-model verification. This procedure ensures that the resulting dataset captures genuine failures of contextual faithfulness.

Parametric Knowledge Elicitation. We adopt a closed-book QA setup and apply a self-consistency mechanism [49, 35] to robustly capture the model’s parametric knowledge. Specifically, we prompt the model n times with the same query and designate the most frequently generated answer (i.e., the majority answer, denoted as \hat{r}) as its dominant belief. Queries for which the majority answer appears fewer than $n/2$ times are discarded to ensure consistency and reliability. Appendix A.6 provides evidence that higher self-consistency improves the quality of faithfulness assessment.

Conflict Detection. To identify whether the model’s parametric knowledge contradicts the external evidence, we compare the dominant answer \hat{r} with the ground-truth answer and the retrieved context. Two advanced pretrained LLMs—GPT-4o [39] and GLM-4-plus [17]—are used to assess whether a conflict exists. To mitigate model-specific bias, only instances where both models agree on the presence of a conflict are retained. Based on this judgment, we assign a faithfulness label $y_f \in \{0, 1\}$, where $y_f = 0$ indicates that \hat{r} conflicts with the context, and $y_f = 1$ otherwise. Appendix A.4 details the implementation procedure. Furthermore, we manually verify a subset of the detected conflicts to confirm their validity against human annotations (see Appendix A.5).

Dataset	#Full*	#Faith.	#Unfaith.
HotpotQA	5,901	1,546	1,427
NewsQA	4,212	374	886
NQ	7,314	3,010	572
SearchQA	16,980	10,692	1,441
SQuAD	10,490	2,799	2,225
TriviaQA	7,785	5,887	767

Table 1: Statistics of the CoFaithfulQA dataset. **#Full*** denotes the number of deduplicated examples from the original dataset. **#Faith.** and **#Unfaith.** indicate the number of samples labeled as faithful and unfaithful, corresponding to \mathcal{D}^+ and \mathcal{D}^- , respectively.

5 Experimental Methodology

This section describes datasets, evaluation metrics, baselines and implementation details.

Datasets. We evaluate the contextual faithful generation performance of different models on the subset \mathcal{D}^- of CoFaithfulQA, as \mathcal{D}^+ samples are already contextually faithful and thus less informative for evaluation. To ensure a comprehensive evaluation, we also include the ConFiQA benchmark [1] as an out-of-domain test set. ConFiQA focuses on evaluating contextual faithfulness in counterfactual scenarios and includes three subsets: Question Answering, Multi-hop Reasoning, and Multi-Conflicts, each containing 6,000 carefully constructed instances.

Evaluation. Following Longpre et al. [34], we adopt a suite of metrics to evaluate the contextual faithfulness of model outputs. To ensure comparability, both generated responses and reference answers are normalized using the approach of Li et al. [32]. We report two primary metrics: context recall ($\text{ConR}\uparrow$), which reflects the degree to which the model’s responses align with the provided external context, and memory recall ($\text{MemR}\downarrow$), which indicates reliance on the model’s internal parametric knowledge. To further characterize the model’s preference between these two sources, we also report the memorization ratio, defined as $\text{MR} = \frac{\text{MemR}}{\text{MemR} + \text{ConR}}$, which quantifies the model’s relative tendency to favor memorized content over retrieved evidence.

Baselines. We evaluate ParamMute against a range of competitive baselines, categorized into four groups: (1) *Prompt-based approaches*, including the attributed prompt ($\text{Attr}_{\text{prompt}}$) and the combined opinion-based and instruction-based prompt ($\text{O\&I}_{\text{prompt}}$) from Zhou et al. [63]; (2) *Decoding-based methods*, where we select the representative COIECD [60], which incorporates entropy-based constraints to perform context-aware contrastive decoding; (3) *Fine-tuning methods*, consisting of standard Supervised Fine-Tuning (SFT) and Knowledge Aware Fine-Tuning (KAFT) [31]. KAFT enhances context faithfulness through counterfactual data augmentation; and (4) *Alignment-based methods*, including Context-DPO (C-DPO) [1], which applies the DPO framework [40] to encourage context-grounded responses while penalizing reliance on parametric memory, and DDR [32], which incorporates differentiable data rewards to train models to better use contextual knowledge.

Implementation Details. To ensure a fair comparison, we use LLaMA3-8B-Instruct as the backbone model for all methods throughout our experiments. For ParamMute, we set the number of UA-FFNs to be suppressed to $N = 8$, and the suppression coefficient in Eq. 11 to 0.0. The hyperparameters α and β , which balance \mathcal{L}_{KAT} and \mathcal{L}_{KPO} in Eq. 8, are both set to 0.5. The impact of different hyperparameter choices is analyzed in Appendix A.9. Additional implementation details for both our method and the baselines are provided in Appendix A.7, and results for different backbone models are reported in Appendix A.12.

6 Experiment Results

In this section, we first present the overall performance of ParamMute, followed by a comprehensive ablation study and an analysis of how ParamMute calibrates the knowledge usage of LLMs.

6.1 Main Results

This experiment evaluates ParamMute on CoFaithfulQA to assess its overall performance. Additionally, we test ParamMute on the ConFiQA dataset, which represents an out-of-domain setting.

As shown in Table 2, ParamMute significantly outperforms baseline models on CoFaithfulQA, demonstrating its effectiveness in generating more accurate and contextually faithful responses. Compared to the vanilla RAG model, ParamMute achieves an average improvement of 5% in ConR and reduces MemR by 4%, effectively mitigating the model’s reliance on parametric knowledge and encouraging better utilization of external context. The evaluation results also indicate that prompt-based methods and decoding-based approaches such as $\text{Attr}_{\text{prompt}}$, $\text{O\&I}_{\text{prompt}}$, and COIECD decrease the MemR score, showing their effectiveness in reducing the model’s reliance on parametric knowledge. However, they also lead to a decline in answer correctness, as reflected by lower ConR score compared to the Vanilla RAG model. In contrast, fine-tuning-based approaches, such as SFT, KAFT, DPO, and DDR, enhance contextual faithfulness by adjusting the parameters of LLMs, highlighting the crucial role these parameters play in the emergence of knowledge conflicts within the

Models	HotPotQA			NQ			NewsQA		
	ConR \uparrow	MemR \downarrow	MR \downarrow	ConR \uparrow	MemR \downarrow	MR \downarrow	ConR \uparrow	MemR \downarrow	MR \downarrow
Vanilla-RAG [42]	60.34	13.88	18.70	53.09	14.41	21.35	60.27	8.24	12.03
Attr _{prompt} [63]	58.93	13.95	19.13	55.36	11.07	16.67	58.80	7.56	11.39
O&I _{prompt} [63]	47.79	10.72	18.32	49.25	8.23	14.32	52.03	5.30	9.25
COIECD [60]	62.51	12.19	16.32	56.21	12.28	17.93	51.81	6.21	10.70
SFT [51]	70.92	<u>6.24</u>	8.08	59.76	10.29	14.69	61.96	5.08	7.58
KAFT [31]	69.52	6.87	8.99	60.89	9.23	<u>13.16</u>	65.09	4.74	6.79
C-DPO [1]	67.20	7.64	10.21	<u>62.24</u>	9.79	<u>13.6</u>	61.4	4.74	7.17
DDR [32]	68.66	7.15	9.43	63.29	10.33	14.03	64.74	5.03	7.21
ParamMute	71.06	6.17	7.99	60.68	<u>9.08</u>	13.02	65.24	<u>4.85</u>	<u>6.92</u>
Models	SearchQA			SQuAD			TriviaQA		
	ConR \uparrow	MemR \downarrow	MR \downarrow	ConR \uparrow	MemR \downarrow	MR \downarrow	ConR \uparrow	MemR \downarrow	MR \downarrow
Vanilla-RAG [42]	66.76	10.55	13.64	77.93	6.79	8.01	61.80	11.47	15.66
Attr _{prompt} [63]	62.53	10.55	14.43	77.35	6.38	7.62	59.97	10.43	14.81
O&I _{prompt} [63]	52.26	9.23	15.01	76.81	6.11	7.37	55.41	8.08	12.73
COIECD [60]	69.74	11.66	14.32	73.12	7.64	9.46	63.62	11.99	15.86
SFT [51]	75.29	6.87	8.36	79.19	4.22	5.06	59.6	8.34	12.38
KAFT [31]	77.38	7.43	8.76	80.04	4.18	4.96	<u>62.32</u>	8.74	12.29
C-DPO [1]	64.12	5.62	8.06	80.08	5.26	6.16	58.67	8.74	12.96
DDR [32]	78.07	6.48	<u>7.66</u>	81.36	4.75	5.52	60.71	<u>7.73</u>	<u>11.29</u>
ParamMute	78.76	<u>6.04</u>	7.12	<u>80.58</u>	4.04	4.78	60.89	6.91	10.19

Table 2: Performance on the CoFaithfulQA dataset. The highest scores are highlighted in **bold**, while the second-highest scores are underlined.

Models	Question Answering			Multi-hop Reasoning			Multi-Conflicts		
	ConR \uparrow	MemR \downarrow	MR \downarrow	ConR \uparrow	MemR \downarrow	MR \downarrow	ConR \uparrow	MemR \downarrow	MR \downarrow
Vanilla-RAG [42]	26.24	38.51	59.47	14.87	24.98	62.69	4.49	13.53	75.09
Attr _{prompt} [63]	47.33	25.78	35.26	17.69	22.42	55.90	6.60	14.67	68.97
O&I _{prompt} [63]	66.22	13.69	17.13	16.78	17.18	50.59	11.64	12.60	51.97
COIECD [60]	71.69	15.33	17.62	53.36	17.13	24.31	57.11	9.60	14.39
SFT [51]	78.02	<u>5.02</u>	<u>6.05</u>	61.40	<u>13.47</u>	17.99	61.98	9.54	13.34
KAFT [31]	82.04	5.58	6.36	63.71	13.64	<u>17.63</u>	67.31	9.98	12.91
C-DPO [1]	81.82	6.20	7.04	58.89	14.00	<u>19.21</u>	58.24	8.71	13.01
DDR [32]	80.71	6.07	6.99	60.64	15.60	20.46	61.07	<u>8.93</u>	<u>12.76</u>
ParamMute	81.20	3.69	4.35	63.09	12.82	16.89	65.20	9.29	12.47

Table 3: Performance of different models on the testing sets of ConFiQA.

models. ParamMute usually shows better performance than these fine-tuning based methods, which thrives on its “suppression-and-adaptation” mechanism.

To further evaluate the generalization capability of ParamMute, we evaluate it on the ConFiQA benchmark. As shown in Table 3, ParamMute outperforms both prompt-based and fine-tuning-based methods in both contextual faithfulness and reducing reliance on parametric knowledge, demonstrating strong generalization ability. These improvements highlight the effectiveness of ParamMute in encouraging LLMs to rely on contextual evidence rather than internal memorization.

6.2 Understanding ParamMute via Ablation and Component Analysis

We conduct ablation studies to analyze the effectiveness of ParamMute’s suppression strategy and to evaluate the contributions of its key components. Specifically, we compare suppression across different model sublayers, examine alternative FFN selection strategies, and assess the individual impact of the suppression and adaptation modules.

Are FFNs the Primary Drivers of Unfaithful Generation? To assess the contribution of different transformer components to unfaithful generation, we evaluate different suppression strategies. In addition to suppressing the UA-FFNs sublayers identified by ParamMute, we evaluate three alternatives: suppressing multi-head attention sub-layers (MHA), suppressing knowledge-related parameters (Parameter) [28], and suppressing entire transformer layers (Layer). All strategies share the same implementation setup, except for the specific component being suppressed. Technical details are

provided in Appendix A.10. As shown in Table 4 (rows 3–6), ParamMute yields the most significant improvements in contextual faithfulness. This suggests that FFN sublayers play a more central role in parametric knowledge recall than other components, consistent with prior findings that position FFNs as key repositories of internal memory [7, 16].

Can Other FFNs Match the Effect of Those Selected by ParamMute? To assess whether alternative FFN selections can achieve similar improvements in contextual faithfulness, we compare ParamMute with several variants that suppress different subsets of FFNs. Specifically, we experiment with suppressing FFNs in bottom layers, mid layers, and randomly selected layers, as detailed in Table 4 (rows 8–11). Our results show that suppressing bottom-layer FFNs leads to a substantial drop in ConR, indicating poor contextual grounding. Mid-layer and randomly selected FFNs suppressing methods yield moderately better performance, but still underperform ParamMute. These findings highlight the crucial role of the FFNs identified by ParamMute, underscoring their effectiveness in mitigating parametric knowledge reliance and improving contextual faithfulness.

Contributions of Different Components of ParamMute. As shown in Table 4 (rows 13–15), we compare ParamMute with two ablated variants:

ParamMute w/o Suppression and ParamMute w/o Adaptation, in order to examine the contributions of each component. Removing the suppression module results in an increase of approximately 0.8% in MemR, suggesting that suppressing activation is effective in reducing reliance on parametric knowledge. In contrast, removing the Adaptation module leads to a 1% drop in ConR, highlighting its role in promoting better use of external context. These findings confirm the effectiveness of ParamMute in reducing the dependence of LLMs on internal memory for faithful generation.

Method	ConR ↑	MemR ↓	MR ↓
<i>Suppressed Component Selection</i>			
FFN	69.54	6.18	8.34
MHA	68.35	6.81	9.23
Layer	62.52	6.03	8.92
Parameter	68.71	6.67	8.85
<i>Suppressed Layer Selection</i>			
UA-FFNs	69.54	6.18	8.34
Bottom	62.29	7.15	10.38
Middle	67.11	6.85	9.43
Random	67.65	7.20	9.84
<i>Faithful Enhancement Strategies</i>			
ParamMute	69.54	6.18	8.34
w/o Suppression	69.47	7.01	9.34
w/o Adaption	68.57	6.32	8.58

Table 4: Comparison of suppression strategies in ParamMute, covering component-level and layer-level variants, along with ablation studies on suppression and adaptation components.

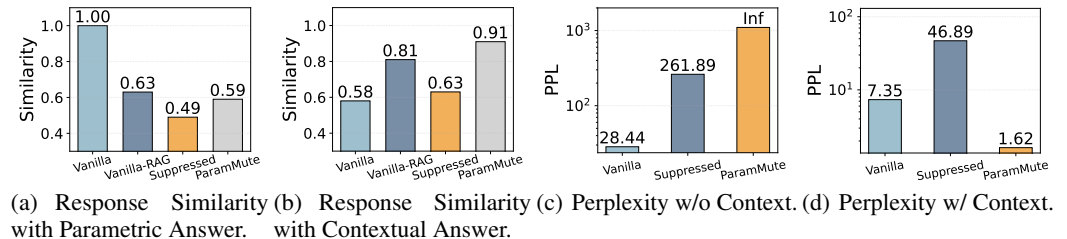


Figure 2: Evaluation of knowledge utilization of different models. We assess the response similarity with parametric answer and contextual answer (Figure 2(a) and Figure 2(b)), and compute the PPL score when reproducing the ground truth answer (Figure 2(c) and Figure 2(d)). The Suppressed model refers to ParamMute w/o Adaption, which only incorporates the knowledge suppression.

6.3 Effectiveness of ParamMute in Calibrating Knowledge Usage Behavior

To assess whether ParamMute improves contextual faithfulness by guiding LLMs to favor retrieved evidence over incorrect internal knowledge, we conduct a comparative analysis on \mathcal{D}^- , the unfaithful subset of CoFaithfulQA. We compare the performance of three models: the vanilla LLM, the Suppressed model (ParamMute w/o Adaptation), and our ParamMute.

We first evaluate the model’s knowledge usage preference by computing the semantic similarity between its outputs and two reference answers: (1) the parametric answer \hat{r} , representing the model’s internal belief obtained in a closed-book setting (Section 4), and (2) the contextual answer y^* derived from retrieved evidence. As shown in Figure 2(a), the Suppressed model achieves the lowest similarity to parametric answers, indicating that activation suppression effectively weakens reliance on internal knowledge. Meanwhile, Figure 2(b) shows that ParamMute achieves the highest similarity with

contextual answers, indicating the effectiveness of ParamMute in enhancing the context knowledge usage ability of LLMs by using a plug-and-play knowledge adaptation module.

To further assess knowledge calibration, we measure the perplexity (PPL) of each model when reproducing the ground-truth answer, both with and without contextual input. A lower PPL indicates greater confidence in generating the correct response. Figure 2(c) shows that when no context is provided, the Suppressed model exhibits a higher PPL, confirming its effectiveness in reducing the dependence on parametric memory. Alternatively, ParamMute displays extremely high PPL in the absence of context but significantly lower PPL when context is available (Figure 2(d)), confirming that the model has shifted to reliance primarily on retrieved evidence instead of the parametric knowledge.

7 Related work

Despite considerable advancements of Retrieval-Augmented Generation (RAG) models [42, 44, 57], unfaithful generation [20]—where models produce content that is not supported by, or even contradicts, the retrieved external evidence—remains a critical and persistent challenge. Even when supplied with accurate and relevant external knowledge, RAG models frequently prioritize their internal parametric knowledge over retrieved information, leading to unfaithful outputs and diminishing the reliability of such systems [3, 5, 34, 58, 53]. Thus, the demand for contextually faithful LLMs has significantly increased, particularly within RAG applications [4, 30].

Numerous studies have systematically investigated this phenomenon from both evaluation and analytical perspectives. For instance, certain research constructs synthetic scenarios by manually replacing entities in retrieved passages, highlighting the propensity of LLMs to generate responses aligned with their internal knowledge rather than provided external evidence [23, 34]. Other studies demonstrate that LLMs often opt for contextually plausible but internally memorized information when faced with conflicting sources, underscoring the difficulty of overcoming ingrained parametric knowledge biases [26, 53]. Additionally, Jin et al. [24] identifies separate context and memory attention heads, which respectively attend to external and internal sources of information, offering a more granular view into the mechanisms that underlie unfaithful generation. Complementarily, Sun et al. [46] suggest that certain FFNs within LLMs act as knowledge injectors, amplifying the influence of internal memory within the residual stream and thereby contributing to unfaithful generation.

Efforts to improve contextual faithfulness primarily focus on enhancing external knowledge integration through various strategies. One direction focuses on prompt design to guide models toward context-grounded responses [50, 63]. Another approach encompasses fine-tuning LLMs on knowledge-augmented datasets, reinforcing the model’s preference for retrieved information over internal memory [12, 31, 36, 38]. Alignment techniques have also been explored, aiming to encourage external grounding while suppressing dependence on internal parametric knowledge [1, 32]. Moreover, contrastive decoding methods have been proposed, explicitly differentiating between faithful and hallucinated responses to promote alignment with external evidence during generation [2, 43, 23]. Beyond external interventions, prior work [24, 46] has also highlighted the role of internal components such as FFNs in shaping model behavior. Building on this, our work analyzes FFN activation patterns to identify over-active layers strongly correlated with unfaithful outputs. We propose a suppression-based strategy to reduce their influence and enhance contextual grounding.

8 Conclusion

In this paper, we introduce ParamMute, a novel framework designed to enhance the contextual faithfulness of LLMs. Our approach addresses the persistent challenge of LLMs favoring internal parametric knowledge over retrieved evidence. ParamMute first mitigates this over-reliance by strategically suppressing the activation of specific FFNs that exhibit a strong correlation with unfaithful generation. To further promote adherence to external information, ParamMute incorporates a plug-and-play adaptation module that reinforces the model’s grounding in the retrieved content. Additionally, we introduce CoFaithfulQA, a comprehensive benchmark constructed from six diverse QA datasets, enabling controlled evaluation of faithfulness under conflicting knowledge settings. Extensive experiments on CoFaithfulQA and ConFiQA demonstrate that ParamMute significantly enhances generation faithfulness while substantially mitigating dependence on internal knowledge.

References

- [1] Baolong Bi, Shaohan Huang, Yiwei Wang, Tianchi Yang, Zihan Zhang, Haizhen Huang, Lingrui Mei, Junfeng Fang, Zehao Li, Furu Wei, et al. Context-dpo: Aligning language models for context-faithfulness. *ArXiv preprint*, 2024. URL <https://doi.org/10.48550/arXiv.2412.15280>.
- [2] Baolong Bi, Shenghua Liu, Lingrui Mei, Yiwei Wang, Pengliang Ji, and Xueqi Cheng. Decoding by contrasting knowledge: Enhancing llms' confidence on edited facts. *ArXiv preprint*, 2024. URL <https://doi.org/10.48550/arXiv.2405.11613>.
- [3] Baolong Bi, Shenghua Liu, Yiwei Wang, Lingrui Mei, Junfeng Fang, Hongcheng Gao, Shiyu Ni, and Xueqi Cheng. Is factuality enhancement a free lunch for llms? better factuality can lead to worse context-faithfulness. *Authorea Preprints*, 2024.
- [4] Yupeng Chang, Xu Wang, Jindong Wang, Yuan Wu, Linyi Yang, Kaijie Zhu, Hao Chen, Xiaoyuan Yi, Cunxiang Wang, Yidong Wang, et al. A survey on evaluation of large language models. *ACM transactions on intelligent systems and technology*, 15(3):1–45, 2024.
- [5] Hung-Ting Chen, Michael J. Q. Zhang, and Eunsol Choi. Rich knowledge sources bring complex knowledge conflicts: Recalibrating models to reflect conflicting evidence. In *Proceedings of the 2022 Conference on Empirical Methods in Natural Language Processing, EMNLP 2022, Abu Dhabi, United Arab Emirates, December 7-11, 2022*, pages 2292–2307, 2022. URL <https://doi.org/10.18653/v1/2022.emnlp-main.146>.
- [6] Jacob Cohen. A coefficient of agreement for nominal scales. *Educational and psychological measurement*, 20(1):37–46, 1960.
- [7] Damai Dai, Li Dong, Yaru Hao, Zhifang Sui, Baobao Chang, and Furu Wei. Knowledge neurons in pretrained transformers. In *Proceedings of the 60th Annual Meeting of the Association for Computational Linguistics (Volume 1: Long Papers), ACL 2022, Dublin, Ireland, May 22-27, 2022*, pages 8493–8502, 2022. URL <https://doi.org/10.18653/v1/2022.acl-long.581>.
- [8] Herbert Aron David. *The method of paired comparisons*, volume 12. 1963.
- [9] Matthew Dunn, Levent Sagun, Mike Higgins, V Ugur Guney, Volkan Cirik, and Kyunghyun Cho. Searchqa: A new q&a dataset augmented with context from a search engine. *ArXiv preprint*, 2017. URL <http://arxiv.org/abs/1704.05179>.
- [10] Yanai Elazar, Nora Kassner, Shauli Ravfogel, Abhilasha Ravichander, Eduard H. Hovy, Hinrich Schütze, and Yoav Goldberg. Measuring and improving consistency in pretrained language models. *Trans. Assoc. Comput. Linguistics*, 9:1012–1031, 2021. URL https://doi.org/10.1162/tacl_a_00410.
- [11] Yuchun Fan, Yongyu Mu, Yilin Wang, Lei Huang, Junhao Ruan, Bei Li, Tong Xiao, Shujian Huang, Xiaocheng Feng, and Jingbo Zhu. SLAM: towards efficient multilingual reasoning via selective language alignment. In *Proceedings of the 31st International Conference on Computational Linguistics, COLING 2025, Abu Dhabi, UAE, January 19-24, 2025*, pages 9499–9515, 2025. URL <https://aclanthology.org/2025.coling-main.637/>.
- [12] Tianqing Fang, Zhaowei Wang, Wenxuan Zhou, Hongming Zhang, Yangqiu Song, and Muhan Chen. Getting sick after seeing a doctor? diagnosing and mitigating knowledge conflicts in event temporal reasoning. In *Findings of the Association for Computational Linguistics: NAACL 2024, Mexico City, Mexico, June 16-21, 2024*, pages 3846–3868, 2024. URL <https://doi.org/10.18653/v1/2024.findings-naacl.244>.
- [13] Javier Ferrando, Gabriele Sarti, Arianna Bisazza, and Marta R Costa-Jussà. A primer on the inner workings of transformer-based language models. *ArXiv preprint*, 2024.
- [14] Adam Fisch, Alon Talmor, Robin Jia, Minjoon Seo, Eunsol Choi, and Danqi Chen. MRQA 2019 shared task: Evaluating generalization in reading comprehension. In *Proceedings of the 2nd Workshop on Machine Reading for Question Answering, MRQA@EMNLP 2019, Hong Kong, China, November 4, 2019*, pages 1–13, 2019. URL <https://doi.org/10.18653/v1/D19-5801>.
- [15] Mor Geva, Roei Schuster, Jonathan Berant, and Omer Levy. Transformer feed-forward layers are key-value memories. In *Proceedings of the 2021 Conference on Empirical Methods in Natural Language Processing, EMNLP 2021, Virtual Event / Punta Cana, Dominican Republic, 7-11 November, 2021*, pages 5484–5495, 2021. URL <https://doi.org/10.18653/v1/2021.emnlp-main.446>.

- [16] Mor Geva, Avi Caciularu, Kevin Ro Wang, and Yoav Goldberg. Transformer feed-forward layers build predictions by promoting concepts in the vocabulary space. In *Proceedings of the 2022 Conference on Empirical Methods in Natural Language Processing, EMNLP 2022, Abu Dhabi, United Arab Emirates, December 7-11, 2022*, pages 30–45, 2022. URL <https://doi.org/10.18653/v1/2022.emnlp-main.3>.
- [17] Team GLM, Aohan Zeng, Bin Xu, Bowen Wang, Chenhui Zhang, Da Yin, Diego Rojas, Guanyu Feng, Hanlin Zhao, Hanyu Lai, Hao Yu, Hongning Wang, Jiadai Sun, Jiajie Zhang, Jiale Cheng, Jiayi Gui, Jie Tang, Jing Zhang, Juanzi Li, Lei Zhao, Lindong Wu, Lucen Zhong, Mingdao Liu, Minlie Huang, Peng Zhang, Qinkai Zheng, Rui Lu, Shuaiqi Duan, Shudan Zhang, Shulin Cao, Shuxun Yang, Weng Lam Tam, Wenyi Zhao, Xiao Liu, Xiao Xia, Xiaohan Zhang, Xiaotao Gu, Xin Lv, Xinghan Liu, Xinyi Liu, Xinyue Yang, Xixuan Song, Xunkai Zhang, Yifan An, Yifan Xu, Yilin Niu, Yuantao Yang, Yueyan Li, Yushi Bai, Yuxiao Dong, Zehan Qi, Zhaoyu Wang, Zhen Yang, Zhengxiao Du, Zhenyu Hou, and Zihan Wang. Chatglm: A family of large language models from glm-130b to glm-4 all tools, 2024.
- [18] Sachin Goyal, Christina Baek, J Zico Kolter, and Aditi Raghunathan. Context-parametric inversion: Why instruction finetuning may not actually improve context reliance. *ArXiv preprint*, 2024.
- [19] Edward J. Hu, Yelong Shen, Phillip Wallis, Zeyuan Allen-Zhu, Yuanzhi Li, Shean Wang, Lu Wang, and Weizhu Chen. Lora: Low-rank adaptation of large language models. In *The Tenth International Conference on Learning Representations, ICLR 2022, Virtual Event, April 25-29, 2022*, 2022. URL <https://openreview.net/forum?id=nZeVKeeFYf9>.
- [20] Lei Huang, Weijiang Yu, Weitao Ma, Weihong Zhong, Zhangyin Feng, Haotian Wang, Qianglong Chen, Weihua Peng, Xiaocheng Feng, Bing Qin, et al. A survey on hallucination in large language models: Principles, taxonomy, challenges, and open questions. *ArXiv preprint*, 2023. URL <https://doi.org/10.48550/ArXiv.2311.05232>.
- [21] Lei Huang, Xiaocheng Feng, Weitao Ma, Yuchun Fan, Xiachong Feng, Yangfan Ye, Weihong Zhong, Yuxuan Gu, Baoxin Wang, Dayong Wu, et al. Improving contextual faithfulness of large language models via retrieval heads-induced optimization. *ArXiv preprint*, 2025.
- [22] Pengcheng Huang, Mu Yongyu, Wu Yuzhang, Li Bei, Xiao Chunyang, Xiao Tong, and Jingbo Zhu. Translate-and-revise: Boosting large language models for constrained translation. In *Proceedings of the 23rd Chinese National Conference on Computational Linguistics (Volume 1: Main Conference)*, 2024.
- [23] Zhuoran Jin, Pengfei Cao, Yubo Chen, Kang Liu, Xiaojian Jiang, Jiebin Xu, Qixia Li, and Jun Zhao. Tug-of-war between knowledge: Exploring and resolving knowledge conflicts in retrieval-augmented language models. In *Proceedings of the 2024 Joint International Conference on Computational Linguistics, Language Resources and Evaluation, LREC/COLING 2024, 20-25 May, 2024, Torino, Italy*, pages 16867–16878, 2024. URL <https://aclanthology.org/2024.lrec-main.1466>.
- [24] Zhuoran Jin, Pengfei Cao, Hongbang Yuan, Yubo Chen, Jiebin Xu, Huajun Li, Xiaojian Jiang, Kang Liu, and Jun Zhao. Cutting off the head ends the conflict: A mechanism for interpreting and mitigating knowledge conflicts in language models. In *Findings of the Association for Computational Linguistics, ACL 2024, Bangkok, Thailand and virtual meeting, August 11-16, 2024*, pages 1193–1215, 2024. URL <https://doi.org/10.18653/v1/2024.findings-acl.70>.
- [25] Mandar Joshi, Eunsol Choi, Daniel S. Weld, and Luke Zettlemoyer. Triviaqa: A large scale distantly supervised challenge dataset for reading comprehension. In *Proceedings of the 55th Annual Meeting of the Association for Computational Linguistics, ACL 2017, Vancouver, Canada, July 30 - August 4, Volume 1: Long Papers*, pages 1601–1611, 2017. URL <https://doi.org/10.18653/v1/P17-1147>.
- [26] Evgenii Kortukov, Alexander Rubinstein, Elisa Nguyen, and Seong Joon Oh. Studying large language model behaviors under context-memory conflicts with real documents. In *First Conference on Language Modeling*, 2024.
- [27] Tom Kwiatkowski, Jennimaria Palomaki, Olivia Redfield, Michael Collins, Ankur Parikh, Chris Alberti, Danielle Epstein, Illia Polosukhin, Jacob Devlin, Kenton Lee, et al. Natural questions: a benchmark for question answering research. *Transactions of the Association for Computational Linguistics*, 7:453–466, 2019. URL https://doi.org/10.1162/tacl_a_00276.
- [28] Namhoon Lee, Thalaiyasingam Ajanthan, and Philip H. S. Torr. Snip: single-shot network pruning based on connection sensitivity. In *7th International Conference on Learning Representations, ICLR 2019, New Orleans, LA, USA, May 6-9, 2019*, 2019. URL <https://openreview.net/forum?id=B1VZqjAcYX>.

- [29] Patrick S. H. Lewis, Ethan Perez, Aleksandra Piktus, Fabio Petroni, Vladimir Karpukhin, Naman Goyal, Heinrich Küttler, Mike Lewis, Wen-tau Yih, Tim Rocktäschel, Sebastian Riedel, and Douwe Kiela. Retrieval-augmented generation for knowledge-intensive NLP tasks. In *Advances in Neural Information Processing Systems 33: Annual Conference on Neural Information Processing Systems 2020, NeurIPS 2020, December 6-12, 2020, virtual*, 2020. URL <https://proceedings.neurips.cc/paper/2020/hash/6b493230205f780e1bc26945df7481e5-Abstract.html>.
- [30] Bo Li, Peng Qi, Bo Liu, Shuai Di, Jingen Liu, Jiquan Pei, Jinfeng Yi, and Bowen Zhou. Trustworthy ai: From principles to practices. *ACM Computing Surveys*, 55(9):1–46, 2023.
- [31] Daliang Li, Ankit Singh Rawat, Manzil Zaheer, Xin Wang, Michal Lukasik, Andreas Veit, Felix X. Yu, and Sanjiv Kumar. Large language models with controllable working memory. In *Findings of the Association for Computational Linguistics: ACL 2023, Toronto, Canada, July 9-14, 2023*, pages 1774–1793, 2023. URL <https://doi.org/10.18653/v1/2023.findings-acl.112>.
- [32] Xinze Li, Sen Mei, Zhenghao Liu, Yukun Yan, Shuo Wang, Shi Yu, Zheni Zeng, Hao Chen, Ge Yu, Zhiyuan Liu, et al. Rag-ddr: Optimizing retrieval-augmented generation using differentiable data rewards. *ArXiv preprint*, 2024. URL <https://doi.org/10.48550/ArXiv.2410.13509>.
- [33] Xi Victoria Lin, Xilun Chen, Mingda Chen, Weijia Shi, Maria Lomeli, Richard James, Pedro Rodriguez, Jacob Kahn, Gergely Szilvassy, Mike Lewis, Luke Zettlemoyer, and Wen-tau Yih. RA-DIT: retrieval-augmented dual instruction tuning. In *The Twelfth International Conference on Learning Representations, ICLR 2024, Vienna, Austria, May 7-11, 2024*, 2024. URL <https://openreview.net/forum?id=220Tbutug9>.
- [34] Shayne Longpre, Kartik Perisetla, Anthony Chen, Nikhil Ramesh, Chris DuBois, and Sameer Singh. Entity-based knowledge conflicts in question answering. In *Proceedings of the 2021 Conference on Empirical Methods in Natural Language Processing, EMNLP 2021, Virtual Event/Punta Cana, Dominican Republic, 7-11 November, 2021*, pages 7052–7063, 2021. URL <https://doi.org/10.18653/v1/2021.emnlp-main.565>.
- [35] Marcus J Min, Yangruibo Ding, Luca Buratti, Saurabh Pujar, Gail Kaiser, Suman Jana, and Baishakhi Ray. Beyond accuracy: Evaluating self-consistency of code large language models with identitychain. *ArXiv preprint*, 2023.
- [36] Xianjie Mo, Yang Xiang, Youcheng Pan, Yongshuai Hou, and Ping Luo. Mitigating knowledge conflicts in data-to-text generation via the internalization of fact extraction. In *International Joint Conference on Neural Networks, IJCNN 2024, Yokohama, Japan, June 30 - July 5, 2024*, pages 1–9, 2024. URL <https://doi.org/10.1109/IJCNN60899.2024.10651167>.
- [37] Yongyu Mu, Peinan Feng, Zhiqian Cao, Yuzhang Wu, Bei Li, Chenglong Wang, Tong Xiao, Kai Song, Tongran Liu, Chunliang Zhang, et al. Revealing the parallel multilingual learning within large language models. In *Proceedings of the 2024 Conference on Empirical Methods in Natural Language Processing*, pages 6976–6997, 2024.
- [38] Ella Neeman, Roee Aharoni, Or Honovich, Leshem Choshen, Idan Szpektor, and Omri Abend. Disentqa: Disentangling parametric and contextual knowledge with counterfactual question answering. In *Proceedings of the 61st Annual Meeting of the Association for Computational Linguistics (Volume 1: Long Papers), ACL 2023, Toronto, Canada, July 9-14, 2023*, pages 10056–10070, 2023. URL <https://doi.org/10.18653/v1/2023.acl-long.559>.
- [39] R OpenAI. Gpt-4 technical report. *ArXiv*, pages 2303–08774, 2023. URL <https://doi.org/10.48550/ArXiv.2303.08774>.
- [40] Rafael Rafailov, Archit Sharma, Eric Mitchell, Christopher D. Manning, Stefano Ermon, and Chelsea Finn. Direct preference optimization: Your language model is secretly a reward model. In *Advances in Neural Information Processing Systems 36: Annual Conference on Neural Information Processing Systems 2023, NeurIPS 2023, New Orleans, LA, USA, December 10 - 16, 2023*, 2023. URL http://papers.nips.cc/paper_files/paper/2023/hash/a85b405ed65c6477a4fe8302b5e06ce7-Abstract-Conference.html.
- [41] Pranav Rajpurkar, Jian Zhang, Konstantin Lopyrev, and Percy Liang. Squad: 100, 000+ questions for machine comprehension of text. In *Proceedings of the 2016 Conference on Empirical Methods in Natural Language Processing, EMNLP 2016, Austin, Texas, USA, November 1-4, 2016*, pages 2383–2392, 2016. URL <https://doi.org/10.18653/v1/d16-1264>.

- [42] Ori Ram, Yoav Levine, Itay Dalmedigos, Dor Muhlgay, Amnon Shashua, Kevin Leyton-Brown, and Yoav Shoham. In-context retrieval-augmented language models. *Transactions of the Association for Computational Linguistics*, 11:1316–1331, 2023.
- [43] Weijia Shi, Xiaochuang Han, Mike Lewis, Yulia Tsvetkov, Luke Zettlemoyer, and Wen-tau Yih. Trusting your evidence: Hallucinate less with context-aware decoding. In *Proceedings of the 2024 Conference of the North American Chapter of the Association for Computational Linguistics: Human Language Technologies: Short Papers, NAACL 2024, Mexico City, Mexico, June 16-21, 2024*, pages 783–791, 2024. URL <https://doi.org/10.18653/v1/2024.nacl-short.69>.
- [44] Weijia Shi, Sewon Min, Michihiro Yasunaga, Minjoon Seo, Richard James, Mike Lewis, Luke Zettlemoyer, and Wen-tau Yih. REPLUG: retrieval-augmented black-box language models. In *Proceedings of the 2024 Conference of the North American Chapter of the Association for Computational Linguistics: Human Language Technologies (Volume 1: Long Papers), NAACL 2024, Mexico City, Mexico, June 16-21, 2024*, pages 8371–8384, 2024. URL <https://doi.org/10.18653/v1/2024.nacl-long.463>.
- [45] Chenglei Si, Zhe Gan, Zhengyuan Yang, Shuohang Wang, Jianfeng Wang, Jordan L. Boyd-Graber, and Lijuan Wang. Prompting GPT-3 to be reliable. In *The Eleventh International Conference on Learning Representations, ICLR 2023, Kigali, Rwanda, May 1-5, 2023*, 2023. URL <https://openreview.net/forum?id=98p5x51L5af>.
- [46] Zhongxiang Sun, Xiaoxue Zang, Kai Zheng, Yang Song, Jun Xu, Xiao Zhang, Weijie Yu, and Han Li. Redep: Detecting hallucination in retrieval-augmented generation via mechanistic interpretability. *ArXiv preprint*, 2024.
- [47] Hugo Touvron, Thibaut Lavril, Gautier Izacard, Xavier Martinet, Marie-Anne Lachaux, Timothée Lacroix, Baptiste Rozière, Naman Goyal, Eric Hambro, Faisal Azhar, et al. Llama: Open and efficient foundation language models. *ArXiv preprint*, 2023. URL <https://ArXiv.org/abs/2302.13971>.
- [48] Adam Trischler, Tong Wang, Xingdi Yuan, Justin Harris, Alessandro Sordoni, Philip Bachman, and Kaheer Suleiman. Newsqa: A machine comprehension dataset. In *Proceedings of the 2nd Workshop on Representation Learning for NLP, Rep4NLP@ACL 2017, Vancouver, Canada, August 3, 2017*, pages 191–200, 2017. URL <https://doi.org/10.18653/v1/w17-2623>.
- [49] Xuezhi Wang, Jason Wei, Dale Schuurmans, Quoc Le, Ed Chi, Sharan Narang, Aakanksha Chowdhery, and Denny Zhou. Self-consistency improves chain of thought reasoning in language models. *ArXiv preprint*, 2022.
- [50] Yike Wang, Shangbin Feng, Heng Wang, Weijia Shi, Vidhisha Balachandran, Tianxing He, and Yulia Tsvetkov. Resolving knowledge conflicts in large language models. *ArXiv preprint*, 2023. URL <https://doi.org/10.48550/arXiv.2310.00935>.
- [51] Jason Wei, Maarten Bosma, Vincent Y. Zhao, Kelvin Guu, Adams Wei Yu, Brian Lester, Nan Du, Andrew M. Dai, and Quoc V. Le. Finetuned language models are zero-shot learners. In *The Tenth International Conference on Learning Representations, ICLR 2022, Virtual Event, April 25-29, 2022*, 2022. URL <https://openreview.net/forum?id=gEZrGC0zdqR>.
- [52] Jason Wei, Yi Tay, Rishi Bommasani, Colin Raffel, Barret Zoph, Sebastian Borgeaud, Dani Yogatama, Maarten Bosma, Denny Zhou, Donald Metzler, Ed H. Chi, Tatsunori Hashimoto, Oriol Vinyals, Percy Liang, Jeff Dean, and William Fedus. Emergent abilities of large language models. *Trans. Mach. Learn. Res.*, 2022. URL <https://openreview.net/forum?id=yzkSU5zdwD>.
- [53] Jian Xie, Kai Zhang, Jiangjie Chen, Renze Lou, and Yu Su. Adaptive chameleon or stubborn sloth: Revealing the behavior of large language models in knowledge conflicts. In *The Twelfth International Conference on Learning Representations, ICLR 2024, Vienna, Austria, May 7-11, 2024*, 2024. URL <https://openreview.net/forum?id=auKAUJZM06>.
- [54] Rongwu Xu, Zehan Qi, Zhijiang Guo, Cunxiang Wang, Hongru Wang, Yue Zhang, and Wei Xu. Knowledge conflicts for llms: A survey. In *Proceedings of the 2024 Conference on Empirical Methods in Natural Language Processing, EMNLP 2024, Miami, FL, USA, November 12-16, 2024*, pages 8541–8565, 2024. URL <https://aclanthology.org/2024.emnlp-main.486>.
- [55] Boyang Xue, Weichao Wang, Hongru Wang, Fei Mi, Rui Wang, Yasheng Wang, Lifeng Shang, Xin Jiang, Qun Liu, and Kam-Fai Wong. Improving factual consistency for knowledge-grounded dialogue systems via knowledge enhancement and alignment. In *Findings of the Association for Computational Linguistics: EMNLP 2023, Singapore, December 6-10, 2023*, pages 7829–7844, 2023. URL <https://doi.org/10.18653/v1/2023.findings-emnlp.525>.

- [56] Zhilin Yang, Peng Qi, Saizheng Zhang, Yoshua Bengio, William W. Cohen, Ruslan Salakhutdinov, and Christopher D. Manning. Hotpotqa: A dataset for diverse, explainable multi-hop question answering. In *Proceedings of the 2018 Conference on Empirical Methods in Natural Language Processing, Brussels, Belgium, October 31 - November 4, 2018*, pages 2369–2380, 2018. URL <https://doi.org/10.18653/v1/d18-1259>.
- [57] Shunyu Yao, Jeffrey Zhao, Dian Yu, Nan Du, Izhak Shafran, Karthik R. Narasimhan, and Yuan Cao. React: Synergizing reasoning and acting in language models. In *The Eleventh International Conference on Learning Representations, ICLR 2023, Kigali, Rwanda, May 1-5, 2023*, 2023. URL https://openreview.net/forum?id=WE_vluYUL-X.
- [58] Qinan Yu, Jack Merullo, and Ellie Pavlick. Characterizing mechanisms for factual recall in language models. In *Proceedings of the 2023 Conference on Empirical Methods in Natural Language Processing, EMNLP 2023, Singapore, December 6-10, 2023*, pages 9924–9959, 2023. URL <https://doi.org/10.18653/v1/2023.emnlp-main.615>.
- [59] Zeping Yu and Sophia Ananiadou. Neuron-level knowledge attribution in large language models. 2024. URL <https://aclanthology.org/2024.emnlp-main.191>.
- [60] Xiaowei Yuan, Zhao Yang, Yequan Wang, Shengping Liu, Jun Zhao, and Kang Liu. Discerning and resolving knowledge conflicts through adaptive decoding with contextual information-entropy constraint. In *Findings of the Association for Computational Linguistics, ACL 2024, Bangkok, Thailand and virtual meeting, August 11-16, 2024*, pages 3903–3922, 2024. URL <https://doi.org/10.18653/v1/2024.findings-acl.234>.
- [61] Qinggang Zhang, Shengyuan Chen, Yuanchen Bei, Zheng Yuan, Huachi Zhou, Zijin Hong, Junnan Dong, Hao Chen, Yi Chang, and Xiao Huang. A survey of graph retrieval-augmented generation for customized large language models. *arXiv preprint arXiv:2501.13958*, 2025.
- [62] Wayne Xin Zhao, Kun Zhou, Junyi Li, Tianyi Tang, Xiaolei Wang, Yupeng Hou, Yingqian Min, Beichen Zhang, Junjie Zhang, Zican Dong, et al. A survey of large language models. *ArXiv preprint*, 2023.
- [63] Wenzuan Zhou, Sheng Zhang, Hoifung Poon, and Muhan Chen. Context-faithful prompting for large language models. In *Findings of the Association for Computational Linguistics: EMNLP 2023, Singapore, December 6-10, 2023*, pages 14544–14556, 2023. URL <https://doi.org/10.18653/v1/2023.findings-emnlp.968>.

A Appendix

A.1 License

We present the licenses of the datasets used in this study: Natural Questions (CC BY-SA 3.0 license), NewsQA (MIT License), SearchQA and TriviaQA (Apache License 2.0), HotpotQA and SQuAD (CC BY-SA 4.0 license).

All these licenses and agreements permit the use of their data for academic purposes.

A.2 Ethics Statement

Our data construction process involves prompting LLMs to elicit their internal parametric knowledge in order to investigate the underlying causes of hallucinations in generated outputs. While this approach enables targeted analysis of model behavior, it may lead to the generation of inaccurate or hallucinated contents. To ensure the responsible usage, we strictly limit the distribution of the resulting dataset to academic research purposes. The dataset does not contain any personally identifiable information or offensive material, and all contents are curated in accordance with ethical guidelines for responsible AI research and data sharing.

Additionally, we conducted human evaluations to assess the reliability of the LLMs in identifying knowledge conflicts. Evaluation data was carefully distributed to human evaluators solely for research purposes, ensuring it adheres to ethical standards and contains no content that violates these standards.

A.3 Causal Intervention on UA-FFNs Activation

To establish the causal role of UA-FFNs activation in unfaithful generation, we perform intervention experiments by manipulating the activation strength of the Unfaithfulness-Associated FFNs (UA-FFNs). These FFNs are identified in Section 2 as exhibiting strong correlations with unfaithful outputs. Our goal is to examine whether suppressing or enhancing their activation causally affects the faithfulness of the model’s generation.

Intervention Setup. We conduct our intervention experiments on the CoFaithfulQA using the LLaMA3-8B-Instruct model. Each instance $(q, c, y^*, \hat{r}, y_f) \in \mathcal{D}$ is labeled as faithful ($y_f=1$) or unfaithful ($y_f=0$), allowing us to partition the data into \mathcal{D}^+ and \mathcal{D}^- for subsequent analysis. To modulate the influence of parametric knowledge, we apply a scaling factor λ to the output of the selected UA-FFNs layers:

$$\text{UA-FFN}^l(\mathbf{x}_i^l) = (\lambda \cdot \sigma(\mathbf{K}^l \mathbf{x}_i^l))^T \mathbf{V}^l. \quad (11)$$

Here, λ controls the activation of each UA-FFNs layer: when $\lambda < 1$, the contribution of parametric knowledge is suppressed; when $\lambda > 1$, it is amplified. To evaluate the model’s sensitivity to such interventions, we vary λ across $\{0.0, 0.25, 0.5, 0.75, 1.0, 1.25\}$. The unmodified model with $\lambda = 1.0$ serves as the control group, while all other settings constitute the experimental group.

Evaluation Protocol. We evaluate the effect of suppression on model behavior by computing the average negative log-likelihood (NLL) loss over two disjoint subsets of the dataset: the faithful subset \mathcal{D}^+ and the unfaithful subset \mathcal{D}^- . For each setting of the suppression coefficient $\lambda \in [0.0, 1.0]$, we measure the model’s NLL loss separately on both subsets. The suppression is applied to UA-FFNs with varying λ , where $\lambda = 0.0$ denotes full suppression and $\lambda = 1.0$ corresponds to no suppression.

Results. Figure 3 summarizes the model behavior across a range of suppression coefficients λ . The endpoints, $\lambda = 0.0$ (full suppression) and $\lambda = 1.0$ (no suppression), correspond to the intervention and control settings introduced earlier in Figure 1(c) (Section 2.2).

When evaluated on the unfaithful subset \mathcal{D}^- , the NLL increases monotonically as λ decreases, with the highest value observed under full suppression ($\lambda = 0.0$). This trend indicates that suppressing UA-FFNs activation effectively disrupts the model’s ability to generate unfaithful responses, suggesting

that these FFNs play a functional role in facilitating hallucinated content. Meanwhile, on the faithful subset \mathcal{D}^+ , the NLL also decreases as λ decreases. This trend suggests that suppressing UA-FFNs activation not only avoids harming faithful generation, but may even improve it. A possible explanation is that reducing reliance on parametric knowledge encourages the model to more effectively utilize the retrieved context, resulting in more faithful and confident responses. To further validate this trend, we increase the suppression coefficient to $\lambda = 1.25$, thereby amplifying the activation of UA-FFNs. As shown in Figure 3, this leads to a decrease in NLL on the unfaithful subset \mathcal{D}^- and a moderate increase on the faithful subset \mathcal{D}^+ . These findings further confirm that enhanced activation of UA-FFNs facilitates unfaithful generation.

Results. Figure 3 summarizes the model behavior across a range of λ values. The endpoints— $\lambda = 0.0$ (full suppression) and $\lambda = 1.0$ (no suppression)—correspond to the intervention and control settings shown earlier in Figure 1(c) (Section 2.2). To better understand the effect of suppression strength, we examine model performance on the two subsets separately. For the unfaithful subset \mathcal{D}^- , we observe a consistent increase in NLL loss as λ decreases, with a peak at $\lambda = 0.0$. This monotonic trend confirms that suppressing UA-FFNs activation disrupts the model’s ability to produce hallucinated content, implying that these FFNs play a functional role in facilitating unfaithful generation. In contrast, the loss on the faithful subset \mathcal{D}^+ shows only a mild increase as λ decreases, indicating that UA-FFNs contributes little to the generation when the model relies on retrieved context.

Conclusion. These results provide strong causal evidence that the over-activation of UA-FFNs drives unfaithful generation by injecting parametric knowledge into the output. By suppressing these layers, the model becomes less confident in producing hallucinated content, as reflected in the increased loss on \mathcal{D}^- . This confirms that internal memory representations in LLMs—particularly within specific FFNs—are not merely correlated with unfaithful generation, but actively responsible for their emergence.

Dataset	Full Size*	Consistency	Faithful Subset (\mathcal{D}^+)	Unfaithful Subset (\mathcal{D}^-)
HotpotQA	5,901	2,973 (50%)	1,546 (26%)	1,427 (24%)
NewsQA	4,212	1,260 (30%)	374 (9%)	886 (21%)
NQ	7,314	4,419 (60%)	3,010 (41%)	1,409 (19%)
SearchQA	16,980	12,133 (71%)	10,692 (63%)	1,441 (8%)
SQuAD	10,490	5,024 (48%)	2,799 (27%)	2,225 (21%)
TriviaQA	7,785	6,654 (85%)	5,887 (75%)	767 (10%)

Table 5: Number of instances at each stage in the CoFaithfulQA construction pipeline.

A.4 Details of CoFaithfulQA Construction

In this section, we detail the two main steps in constructing CoFaithfulQA.

Parametric Knowledge Elicitation. To elicit the LLM’s parametric knowledge, we prompt the model in a closed-book setting i.e., without providing any external context. To improve the reliability of the elicited responses, we adopt a consistency-based filtering strategy [55]. For each query q , the model is prompted $n = 5$ times, yielding a set of responses $\{r_1, r_2, \dots, r_5\}$. We identify the majority response \hat{r} as the one that appears most frequently. A query q_i is retained if and only if the frequency of \hat{r} is at least 3 (i.e., appears in ≥ 3 out of 5 responses), thereby filtering out inconsistent generations and ensuring the reliability of the extracted parametric knowledge.

The following prompt template is used to elicit responses from the model:

Prompt for Eliciting Parametric Knowledge

Answer the question `{brevity_instruction}` and provide supporting evidence.
Question: `{question}`

The “`brevity_instruction`” is incorporated to encourage the LLM to produce more concise responses, following the guidance strategy proposed by Kortukov et al. [26].

Conflict Detection. Next, we categorize each instance obtained from the previous step into one of two groups—conflicting or non-conflicting—based on whether the model’s parametric knowledge aligns with the retrieved context. To assess the presence of conflict, we employ LLMs to compare

the parametric answer and the contextual evidence. To mitigate model-specific bias, we adopt a dual-model agreement strategy: a conflict label is only assigned when both GPT-4o [39] and GLM-4-plus [17] agree on its presence. For both models, we use the following prompt:

Prompt for Identifying Conflict Knowledge

You are tasked with evaluating the correctness of a model-generated answer based on the given information.
 Context: *{context}*
 Question: *{question}*
 Contextual Answer: *{contextual_answer}*
 Model-Generated Answer: *{Model-Generated_answer}*
 [Detailed task description...]
 Output Format:
 Evaluate result: (Correct / Partially Correct / Incorrect)

Based on this process, we assign each instance an additional binary label y_f indicating faithfulness: $y_f = 0$ (unfaithful) if the parametric knowledge conflicts with the context, and $y_f = 1$ (faithful) otherwise. The unfaithful subset \mathcal{D}^- is used for downstream evaluation experiments, while the faithful subset \mathcal{D}^+ is used for activation analysis.

A.5 Assessing the Reliability of LLMs in Knowledge Conflict Identification

In this subsection, we conduct a human evaluation to assess the reliability of GPT-4o and GLM-4-plus in identifying knowledge conflicts. This evaluation aims to verify whether LLMs can serve as trustworthy tools for automatically detecting conflicts between different knowledge sources, a critical step in our data construction pipeline.

To ensure broad coverage, we randomly sample 150 instances from each of the six subsets of CoFaithfulQA, resulting in a total of 900 examples that span diverse query types and conflict scenarios. Among them, 100 instances are randomly selected and independently annotated by multiple annotators to compute inter-annotator agreement (IAA). The annotations are conducted by six senior researchers (each holding at least a bachelor’s degree) with backgrounds in computational linguistics and LLM behavior analysis, ensuring high-quality and consistent evaluations.

For each instance, annotators are provided with the question, the contextual answer, the model-generated response, and the corresponding supporting evidence. Unlike binary classification approaches (e.g., NLI-based models), we adopt a more fine-grained evaluation protocol. Annotators are asked to classify each response into one of three categories: *No Conflict*, *Somewhat Conflict*, or *High Conflict*. The detailed annotation instructions are as follows:

Annotation Instruction

You are tasked with determining whether the parametric knowledge of LLMs conflicts with the given context to facilitate the study of knowledge conflicts in large language models.

Each data instance contains the following fields:

Question: *{question}*
 Answers: *{answers}*
 Context: *{context}*
 Parametric_knowledge: *{LLMs' parametric_knowledge }*

The annotation process consists of two steps.

Step 1: Compare the model-generated answer with the ground truth answers, based on the given question and context, to determine whether the model’s parametric knowledge conflicts with the context.

Step 2: Classify the results into one of three categories:

{No Conflict} if the model-generated answer is consistent with the ground truth answers and context,

{Somewhat Conflict} if it is partially inconsistent

{High Conflict} if it significantly contradicts the ground truth answers or context.

Subset	Agreement (%)
HotpotQA	89.4
NewsQA	91.3
NQ	89.2
SearchQA	94.6
SQuAD	87.5
TriviaQA	90.3
Average	90.4

Table 6: Agreement between human annotators and LLMs across different subsets of our CoFaithfulQA benchmark.

To ensure annotators fully understand the task, we first instruct them using a set of five gold-standard examples. Additionally, annotators had access to clarification support throughout the annotation process. We observe strong annotation consistency, with a Cohen’s κ of 0.766 between human annotators, indicating substantial inter-annotator agreement [6]. Table 6 shows the agreement rate between human annotators and LLMs across different subsets. LLMs achieves an average agreement of 90.4% with human judgments, demonstrating strong alignment with expert evaluations. Notably, the majority of disagreement cases occur in borderline *Somewhat Conflict* instances, suggesting that LLMs is particularly reliable in identifying clear-cut conflict or non-conflict cases. These results support the use of LLMs as practical and effective tools for scalable conflict identification.

A.6 Self-Consistency Filtering for Reliable Parametric Knowledge Extraction

In this subsection, we assess the effectiveness of our self-consistency-based filtering method in extracting reliable parametric knowledge from LLMs. The core idea is to filter out unstable model beliefs by leveraging generation consistency: for each query, we prompt the model five times and identify the most frequent answer and its occurrence frequency. Queries with low answer frequency likely reflect uncertain or non-committal model behavior, making them unreliable for evaluating the model’s true reliance on internal knowledge. To quantify this effect, we group data into sub-datasets based on answer frequency, and apply our “Conflict Detection” method to retain only instances where knowledge conflicts are detected. We then evaluate ConR and MemR on each sub-dataset.

As shown in Figure 4, a clear trend emerges: as answer frequency increases, ConR decreases while MemR increases. This suggests that when the model becomes more consistent in its responses, it also tends to rely more heavily on internal (parametric) knowledge, leading to a higher rate of unfaithful generation. Conversely, instances with an answer frequency of 1 exhibit minimal reliance on parametric knowledge (MemR = 3%), indicating that their apparent faithfulness may result from the model’s uncertainty rather than true contextual alignment.

These results validate the importance of consistency-based filtering: only when the model confidently expresses its parametric knowledge can we meaningfully assess and intervene in cases of unfaithful generation. This approach also distinguishes our methodology from prior studies [34, 53], which do not account for the stability of model beliefs.

A.7 Additional Experimental Details

This subsection describes the training prompt, training data, and experimental setup for our study.

Prompts. For all methods except Attr_{prompt} and O&I_{prompt}, we use a simple QA-format prompt template, following Zhou et al. [63].

Base Prompt

{context} Q: {question} ? A: {answer}.

Training Datasets. During the training stage of ParamMute, we construct the training data by randomly sampling 32,580 instances from the combined training sets of the six sub-datasets included in our benchmark, all of which are derived from the MRQA 2019 benchmark [14].

Experimental Setup. In this work, all models are trained for 2,100 steps with a total batch size of 32 and a learning rate of 1e-4. To enhance training efficiency, we implement ParamMute with LoRA [19]. For ParamMute, we set the number of suppressed UA-FFNs layers to $N = 8$, and the suppression coefficient in Eq. 11 is fixed at 0.0. The hyperparameters α and β , which control the relative contributions of \mathcal{L}_{KAT} and \mathcal{L}_{KPO} in Eq. 8, are both set to 0.5. Additionally, we adopt a dynamic γ in \mathcal{L}_{KPO} (Eq. 10), which linearly transitions from an initial margin ($\gamma_0 = 1$) to a final margin ($\gamma^* = 5$) as training progresses. This adaptive strategy gradually reduces the model’s reliance on internal parametric knowledge, encouraging it to rely more on external knowledge. To facilitate faithful evaluation on CoFaithfulQA, we adopt a controlled setting for each dataset—following prior

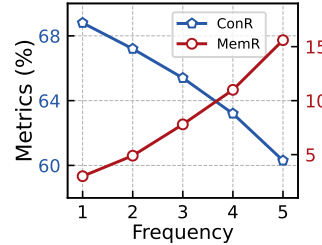


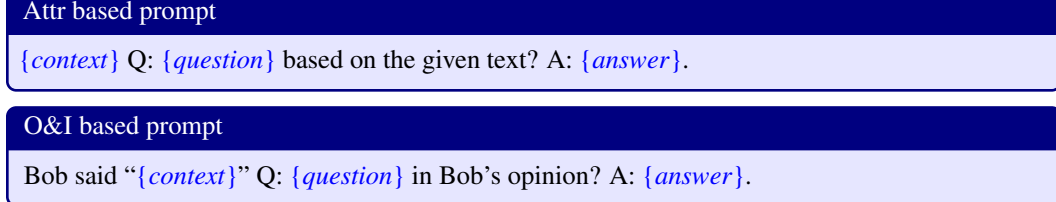
Figure 4: Performance comparison of ConR and MemR across sub-datasets grouped by the answer frequency of LLMs.

works [1, 23, 46]—to ensure that the provided documents are sufficient to answer the questions, thereby isolating the model’s faithfulness from retrieval quality.

A.8 Implementation Details of Baselines

This subsection describes the implementation details of all baseline methods.

We adopt two prompt-based baselines designed to reflect common prompting strategies: the attributed prompt ($\text{Attr}_{\text{prompt}}$), which directly asks the model to state factual knowledge, and the opinion-and-instruction prompt ($\text{O\&I}_{\text{prompt}}$), which combines subjective framing with task-oriented instructions. The corresponding prompt templates are shown below:



For the SFT baseline, we incorporate context during training, similar to ParamMute, while keeping the remaining experimental settings identical. To construct preference pairs for DPO training, we use contextually aligned answers from the dataset as “preferred responses” to ensure the consistency with the provided context. The “rejected responses” are generated by identifying parametric knowledge conflicts through our data construction methodology (§4). For KAFT, we employ a hybrid dataset containing both counterfactual and factual data. Specifically, we integrate the counterfactual data developed by Xie et al. [53], leveraging their advanced data construction framework. For DDR, we follow the strategy described in Li et al. [32] to construct preference data. Specifically, for each training instance, we generate multiple outputs under different decoding conditions by varying the sampling temperature and enabling or disabling the use of retrieved context. Each output is evaluated using an accuracy-based reward function. The responses with the highest and lowest reward scores are selected as the positive and negative samples, respectively, for DPO training.

By maintaining an equivalent dataset size and ensuring comparable data quality across all baselines, we provide a rigorous and fair comparison with our proposed ParamMute.

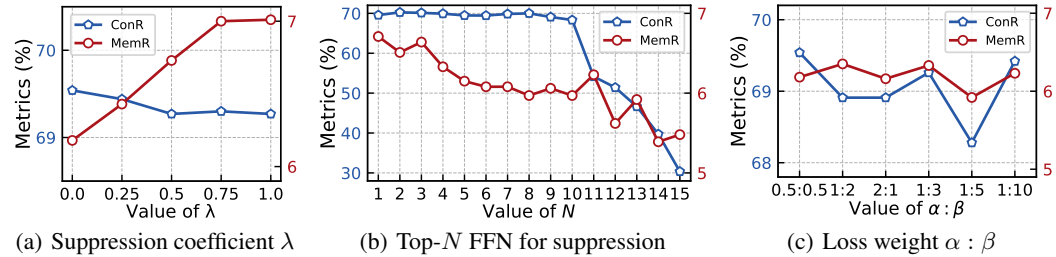


Figure 5: Variation in ConR and MemR under different hyperparameter settings. Each point reflects the average metric across all subsets within CoFaithfulQA. Higher ConR and lower MemR indicate better contextual faithfulness with reduced parametric reliance.

A.9 Impact of Key Hyperparameters in ParamMute

In this section, we analyze the impact of key hyperparameters related to ParamMute. All experimental settings remain consistent with the main implementation of ParamMute, except for the specific hyperparameters under investigation. Specifically, we investigate three factors: (1) the suppression coefficient λ , which controls the strength of activation suppression applied to selected FFNs; (2) the number of top- N FFNs selected for suppression; and (3) the weighting coefficients α and β used to balance the \mathcal{L}_{KAT} and \mathcal{L}_{KPO} during training. The results are presented in Figure 5.

Suppression Coefficient λ . We vary $\lambda \in [0.0, 1.0]$ to analyze the impact of suppression strength applied to UA-FFNs activations, where $\lambda = 0.0$ denotes full suppression and $\lambda = 1.0$ corresponds to

the original model without intervention. As shown in Figure 5(a), decreasing λ consistently reduces MemR and improves ConR, indicating that smaller λ values lead to better contextual faithfulness and reduced reliance on internal memory. At $\lambda = 0.0$, the model achieves the best overall performance. Given its strong effect in promoting contextual faithfulness, we adopt $\lambda = 0.0$ as the default setting in all experiments unless otherwise specified.

The Number of Suppressed FFNs N . We investigate how the number of top-activated FFNs selected for suppression affects the model’s behavior. Specifically, we vary n from 1 to 15, covering nearly half of all FFN layers. As shown in Figure 5(b), increasing n expands the suppression scope and consistently reduces MemR. However, when n reaches 10, we observe a sharp drop in ConR, suggesting that excessive suppression may interfere with functions beyond knowledge storage. This indicates that not all FFN layers are suppressible without adverse effects, and overly broad suppression can impair the model’s ability to utilize external context.

Loss Balancing Coefficients α and β . During joint training, we use α and β to weight Knowledge-Augmented Training (\mathcal{L}_{KAT}) and Knowledge Preference Optimization (\mathcal{L}_{KPO}), respectively. We empirically test different ratios of $\alpha : \beta$ and find that varying this ratio has limited impact on overall performance. Nonetheless, moderate weighting (e.g., $\alpha = 0.5$, $\beta = 1.0$) achieves a good balance between suppressing parametric interference and maintaining task accuracy (see Figure 5(c)).

A.10 Implementation Details of Different Suppression Strategies

This subsection provides implementation details of four suppression strategies designed to reduce the influence of specific model components. These strategies are introduced to investigate how different types of internal suppression affect contextual faithfulness. All methods are applied to the same set of layers identified using the approach in Section 3.1, and implemented on a shared model backbone (LLaMA3-8B-Instruct) to ensure fair comparison. For consistency, we use a uniform suppression coefficient of $\lambda = 0.0$, effectively nullifying the contribution of the targeted submodules.

FFN Suppression (ParamMute). We identify a fixed set of unfaithfulness-associated FFN sublayers (as described in Section 2.2) and suppress them by scaling the hidden activations after the nonlinearity with a suppression coefficient $\lambda = 0.0$ in Eq. 11.

Multi-Head Attention (MHA) Suppression. To suppress attention layers, we select the same number of transformer blocks as in the FFN setting and scale the multi-head attention output by λ .

Parameter Suppression (SNIP-inspired). Following the SNIP criterion [28], we compute a saliency score for each individual parameter within the identified FFN layers, defined as the product of the parameter value and the gradient of the loss with respect to that parameter. We then select the top- k parameters with the highest saliency scores, where k is set to match the total number of parameters suppressed in our FFN suppression strategy. These parameters are suppressed by applying a binary mask matrix scaled by the suppression coefficient λ , effectively modulating their contribution without altering the remaining model weights. This setup aligns the overall suppression magnitude with that of FFN suppression, allowing for a more consistent comparison between strategies.

Layer Suppression. We apply suppression to the same set of transformer blocks used in the FFN suppression strategy. For each selected block, we scale the output of the entire block—comprising both the multi-head attention and FFN submodules—by the suppression coefficient λ during inference. This allows us to assess the impact of suppressing entire transformer layers while keeping the number and location of suppressed blocks consistent across strategies.

A.11 How Activation Strength Shapes Parametric Knowledge Reliance?

To better understand how activation strength affects the model’s reliance on internal parametric knowledge, we conduct experiments under both the zero-shot and knowledge-adapted settings. Specifically, we evaluate Memory Recall (MemR) and

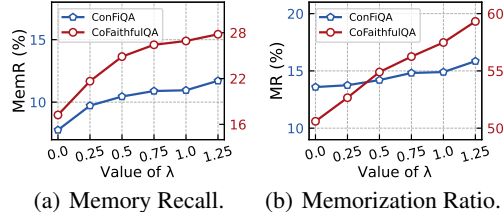


Figure 6: Trends in Memory Recall (MemR) and Memorization Ratio (MR) under varying suppression coefficients λ , evaluated on ConFiQA and CoFaithfulQA. Each point reflects the average metric across all subsets within the respective benchmark.

Memorization Ratio (MR) across a range of suppression coefficients λ on ConFiQA and CoFaithfulQA.

As shown in Figure 6, panels (a)–(b) report results for the original model without fine-tuning. In both cases, we observe that decreasing λ —i.e., applying stronger suppression to UA-FFNs activations—consistently reduces MemR and MR, indicating that suppression effectively reduces reliance on internal parametric memory (lower MemR), without degrading the model’s use of external context, as evidenced by the expected decline in MR with decreasing λ .

These findings empirically highlight the relationship between FFN activation strength and the model’s dependency on parametric knowledge. Moreover, they demonstrate the potential of activation-level control as a mechanism for modulating knowledge reliance, offering practical insights for flexibly balancing internal memory and contextual grounding in downstream applications.

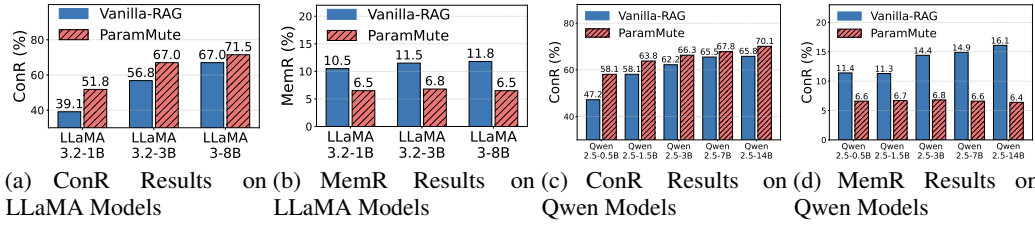


Figure 7: Average ConR and MemR across different models based on the LLaMA and Qwen series, before and after applying ParamMute.

Models	CoFaithfulQA			ConFiQA		
	ConR \uparrow	MemR \downarrow	MR \downarrow	ConR \uparrow	MemR \downarrow	MR \downarrow
LLaMA3-8B	63.37	10.89	14.9	22.52	31.15	59.77
+ParamMute	69.54	6.18	8.34	69.83	8.60	11.24
LLaMA3.1-8B	59.53	10.83	15.84	15.38	29.97	68.98
+ParamMute	68.45	6.65	9.10	71.12	9.01	11.44
LLaMA3.2-1B	35.44	9.63	21.74	32.09	18.32	36.28
+ParamMute	49.79	6.21	11.27	62.70	7.63	11.38
LLaMA3.2-3B	53.13	10.67	17.02	26.16	23.47	49.05
+ParamMute	65.04	6.50	9.28	69.61	8.39	11.09
Qwen2.5-0.5B	43.55	10.50	19.39	50.72	17.15	26.20
+ParamMute	56.17	6.33	10.34	67.54	8.04	11.03
Qwen2.5-1.5B	54.46	10.42	16.39	51.69	19.87	28.23
+ParamMute	61.82	6.44	9.69	69.61	8.35	11.05
Qwen2.5-3B	58.60	13.59	18.79	25.47	29.34	55.70
+ParamMute	64.35	6.45	9.31	66.30	8.62	11.94
Qwen2.5-7B	62.78	13.53	17.79	24.75	33.09	59.04
+ParamMute	65.79	6.30	8.94	69.54	8.85	11.58
Qwen2.5-14B	62.13	15.27	19.66	7.86	32.88	83.71
+ParamMute	68.05	6.13	8.48	71.70	8.90	11.29

Table 7: Average performance of LLMs on CoFaithfulQA and ConFiQA before and after applying ParamMute.

A.12 Extending ParamMute to More LLMs

We extend ParamMute to a diverse range of LLMs, encompassing multiple model families and sizes. Specifically, our evaluation includes LLaMA3-8B-Instruct, LLaMA3.2-1B-Instruct, LLaMA3.2-3B-Instruct, Qwen2.5-0.5B-Instruct, Qwen2.5-1.5B-Instruct, Qwen2.5-3B-Instruct, Qwen2.5-7B-Instruct, and Qwen2.5-14B-Instruct. The results on ConR and MemR are summarized in Figures 7, while Table 7 presents the average performance of all models on CoFaithfulQA and ConFiQA. This comprehensive evaluation demonstrates the versatility and scalability of ParamMute across a wide spectrum of model architectures and sizes.

These experimental results also illustrate several key insights: 1) Larger models tend to rely more on parametric memory. As model size increases in both the LLaMA and Qwen families, MemR also grows, indicating a tendency to overlook external knowledge in favor of internal parameters. ParamMute counteracts this behavior, decreasing larger models’ MemR score to even below that of smaller models. 2) ParamMute consistently benefits all evaluated models. Across both LLaMA and Qwen model families, ParamMute outperforms Vanilla-RAG by boosting accuracy and context faithfulness, underscoring its broad applicability and effectiveness. 3) Not all parameters in RAG models are essential. Pruning parametric knowledge not only reduces computation costs but also fosters better generalization without sacrificing accuracy, highlighting the potential of building a parameter-efficient LLM within the RAG framework.

B Limitations and Societal Impacts

Limitations. While our method demonstrates consistent improvements across multiple benchmarks, several aspects remain open for future exploration.

Firstly, to facilitate the evaluation of faithfulness in retrieval-augmented generation, CoFaithfulQA is constructed under a controlled setting where the retrieved context is guaranteed to contain sufficient information to answer the question. As a result, unfaithful responses caused by retrieval failures are not reflected in this benchmark. We aim to extend the benchmark to cover a diverse range of task scenarios in future work, thus providing a more comprehensive evaluation of contextual faithfulness in LLMs. Secondly, our intervention strategy focuses on suppressing a specific subset of FFN layers based on activation patterns. While effective, this design operates at a relatively coarse granularity. Exploring finer-grained interventions, such as at the level of individual neurons, may yield further gains in controlling parametric knowledge influence. Finally, due to computational constraints, our experiments are conducted on models of moderate scale. Although our findings generalize across multiple model families, future work could investigate whether similar patterns hold in larger-scale models, and whether scaling effects introduce new challenges or opportunities for intervention.

Societal Impacts. Enhancing the faithfulness of retrieval-augmented language models can significantly improve the reliability of AI systems in real-world applications, such as question answering, digital assistants, and knowledge-based services. By reducing the likelihood of generating factually incorrect or misleading responses, our method contributes to safer and more trustworthy deployment of large language models in practice. Furthermore, the proposed activation suppression mechanism offers a flexible means of controlling the model’s reliance on parametric knowledge. This flexibility enables task-specific adaptation—dynamically increasing or decreasing dependence on internal memory according to contextual demands—making our approach potentially beneficial in a wide range of downstream scenarios where different levels of grounding are required, such as healthcare, finance, and scientific research, where factual consistency and evidence alignment are particularly critical.